THE JOURNAL OF PHYSICAL CHEMISTRY B

ARTICLE

pubs.acs.org/JPCB

Structural and Dynamical Insights into the Molten-Globule Form of Ovalbumin

Mily Bhattacharya* and Samrat Mukhopadhyay*

Indian Institute of Science Education and Research (IISER), Mohali, Knowledge City, Sector 81, SAS Nagar, Mohali 140306, India

Supporting Information

ABSTRACT: Ovalbumin is a 45 kDa egg-white glycoprotein which belongs to the class of serpin superfamily. We have studied the structural properties of both native and partially unfolded molten-globule forms of ovalbumin using a diverse array of spectroscopic tools. Time-resolved fluorescence measurements provided important structural and dynamical insights into the native and molten-globule states. Fluorescence anisotropy decay analysis indicated that there is a conformational swelling from the native to the molten-globule form of ovalbumin. We have also carried out red-edge excitation shift measurements to probe the dipolar relaxation dynamics around the intrinsic tryptophan residues. Additionally, stopped-flow fluorescence experiments revealed that the conformational transition from the native to the molten-globule form proceeds in a stepwise manner involving a burst-phase with a submillisecond conformational change followed by biphasic slower conformational reorganizations on the millisecond time scale leading to the final molten-globule state.

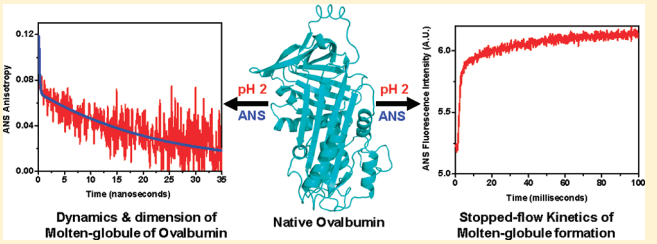

1. INTRODUCTION

The molten-globule state of a protein is defined as a partially unfolded state that retains some degree of secondary structure but is devoid of compact tertiary structure.[1] Such a partially unfolded state, having exposed hydrophobic regions, has been implicated as an important intermediate in both protein folding and protein aggregation processes.[2] It has been conjectured that the partially extended, molten-globule conformers are aggregation-prone and can serve as precursors to protein aggregates and amyloid fibrils that are implicated in a range of protein-misfolding disorders.[3] Recently, there has been considerable interest in the aggregation studies of serpins since serpin misfolding and polymerization, mediated by partially folded intermediates, have been linked to several diseases such as Alzheimer-like dementia, emphysema, liver cirrhosis, etc.[4] Serpins, such as α_1-antitrypsin and antithrombin, are serine protease inhibitors that naturally occur in the stressed, metastable conformation and are involved in many important physiological functions such as blood coagulation, blood pressure regulation, apoptosis, etc.[5] Upon binding to a substrate followed by proteolysis across the reactive center loop, they undergo a conformational change whereby the proteolytically cleaved reactive center loop gets inserted into the central β-sheet and the resulting conformer is more relaxed and thermostable.[6] However, such inherent metastability coupled with mutations has been proposed to lead to the formation of misfolded serpin conformers that eventually polymerize and cause physiological disorders. Therefore, it is important to gain detailed structural insights into the metastable, native serpin and the partially folded intermediates that might play a crucial role in serpinopathies.

Ovalbumin is a 385-residue, 45 kDa model egg-white glycoprotein which belongs to the class of serpin superfamily and is widely used in the food industry as an emulsifier and gelling agent.[7,8] It is composed of nine α-helices and three β-sheets wherein the central β-sheet is oriented parallel to the protein's long axis and the reactive center loop is a short α-helix that is exposed to the environment (Figure 1). Ovalbumin contains three tryptophan residues (Trp 148, Trp 184, Trp 267), four free cysteines (Cys 11, Cys 30, Cys 367, Cys 382), and one solvent-accessible disulfide bond involving cysteine residues at positions 73 and 120.[9] It is well documented that, unlike other serpins, ovalbumin does not play the role of a serine protease inhibitor.[10] Previous reports involving characterization of both disulfide-intact and reduced forms of ovalbumin under native and acidic pH conditions have shown that it forms a molten-globule-like state at pH 2.2.[11−13] Recently, it has been demonstrated that the molten-globule-like state of ovalbumin aggregates under low-pH conditions.[14]

In this paper, we describe a detailed study on the conformational and size changes of various pH-induced conformers of ovalbumin using a variety of biophysical tools. Using intrinsic (tryptophan) and extrinsic (ANS) fluorescent probes as well as circular dichroism, we demonstrate that ovalbumin adopts a molten-globule-like state at low pH. Time-resolved fluorescence measurements provided important dynamical insights into the different conformational states of the protein. We have also

Received: August 31, 2011
Revised: November 8, 2011
Published: November 18, 2011

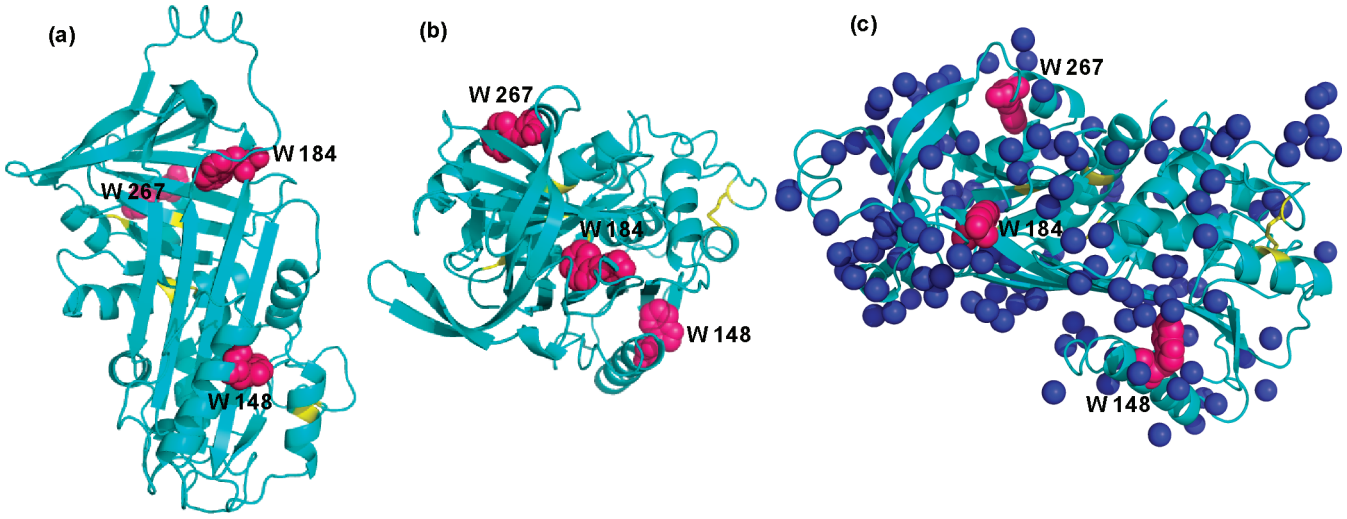

Figure 1. Crystal structure of ovalbumin generated using Pymol (Delano Scientific LLC, CA) from the Protein Data Bank (PDB ID: 1OVA) shown in (a) side view, (b) top view (for a better clarity of the locations of all the three tryptophans), and (c) side view with water molecules. The three tryptophan residues (W148, W184, W267) are shown as magenta spheres, four cysteine residues (C11, C30, C367, C382) as yellow ribbon, a single disulfide bond (C73−C120) as a yellow stick, and water molecules as blue spheres. Ovalbumin is the major constituent of egg-white protein, contains nine α-helices and three β-sheets, and belongs to the serpin superfamily.

investigated the dipolar relaxation of the intrinsic tryptophans in both native and other low-pH conformers using the red-edge excitation shift (REES) approach. Additionally, we have probed the kinetics of conformational transition from the native state to the low-pH form using stopped-flow fluorescence technique that illuminates the mechanism of molten-globule formation.

2. EXPERIMENTAL METHODS

2.1. Materials. Ovalbumin, 8-anilinonaphthalene-1-sulfonic acid (ANS) ammonium salt, Nile Red, glycine, citric acid, potassium chloride, potassium iodide (KI), Tris, sodium phosphate monobasic dihydrate, and sodium phosphate dibasic dihydrate were purchased from Sigma (St. Louis, MO) and used without any further purification. Milli-Q water was used for the preparation of all the solutions and buffers. KCl−HCl (pH 1.6, 2), glycine−HCl (pH 2.5, 3), sodium citrate (pH 3.5−6), sodium phosphate mono- and dibasic dihydrate (pH 6.5−8), Tris−HCl (pH 8.5), and glycine−NaOH (pH 9−10.5) were used for buffer preparations. All the buffers (pH 1.6−10.5) were prepared freshly before every pH titration experiment. The pH of the buffers was checked on a pH 827 lab meter from Metrohm. The final pH was in the range of ±0.01 at 24−25 °C.

2.2. Preparation of Protein Sample. For pH titration experiments, ovalbumin was dissolved in phosphate buffer of pH 7, 5 mM to give a stock solution of 1 mM and stored at 4 °C. Accurate protein concentration was determined by measuring the absorbance of tryptophans at 280 nm on a Lambda 25, Perkin-Elmer UV−visible spectrophotometer. The molar extinction coefficient of ovalbumin at 280 nm is 30 957 M^{-1} cm^{-1}.[14] Typically, 1 mM of ovalbumin in phosphate buffer (pH 7, 5 mM) was diluted 100-fold by using a required buffer (pH 1.6−10.5, 50 mM) to a final protein concentration of 10 μM and kept for 2 h at 25 °C to ensure complete equilibration. All the measurements were carried out at ∼24 °C.

2.3. Preparation of KI Solution. To investigate tryptophan fluorescence quenching during red-edge excitation shift (REES) experiments as a function of pH and quencher concentration, KI was used as the quencher. Typically, a 5 M stock solution of KI containing 250 μM of $Na_2S_2O_3$ was prepared in Milli-Q water at room temperature. For quenching experiments, KI concentration was varied from 100 to 500 mM which was obtained by suitable dilution of the KI stock solution into the protein samples already equilibrated at different pH.

2.4. Steady-State Fluorescence Measurements. All the steady-state fluorescence measurements were performed on an LS 55 luminescence spectrometer from Perkin-Elmer at room temperature (∼24 °C), and the final protein concentration was kept constant at 10 μM. The fluorescence intensity and anisotropy of tryptophans and ANS were measured to probe the conformational and size changes in the monomeric protein conformers. For ANS fluorescence experiments, 10 μM of ANS was used which was obtained by suitable dilution of a stock solution (1 mM) of ANS (prepared in Milli-Q water and stored at 4 °C) into protein solution prior to the ANS intensity and anisotropy measurements. For Nile Red binding experiments, the final concentration of Nile Red was 1 μM. For red-edge excitation shift (REES)-based experiments in the presence of the quencher, an aqueous stock solution of KI was diluted into the protein samples following which the tryptophan spectra were collected at different quencher concentrations and at different excitation wavelengths. For all the experiments, the fluorescence intensity and anisotropy were collected at constant wavelength with an integration time of 5 and 30 s, respectively. The steady-state anisotropy (r_{ss}) is given by

$$r_{ss} = (I_{||} - I_{\perp}G)/(I_{||} + 2I_{\perp}G) \quad (1)$$

where $I_{||}$, $I_{\perp}$ are fluorescence intensities collected using parallel and perpendicular geometry of the polarizers, respectively, and the perpendicular components were corrected using respective G-factors. The error associated with the fluorescence anisotropy measurements was below 0.01. The following parameters were adjusted for monitoring tryptophan fluorescence intensity and anisotropy during pH titration experiments: λ_{ex} = 300 nm, λ_{em} = 350 nm, excitation band pass = 2.5 nm, emission band

dx.doi.org/10.1021/jp208416d |J. Phys. Chem. B 2012, 116, 520–531

pass = 4 nm (for intensity) and 8−10 nm (for anisotropy). For collecting the tryptophan spectral scans during REES and quenching experiments, the parameters were λ_{ex} = 280/290/295/305 nm, λ_{em} (scan range) = 320−400 nm with an excitation and emission band pass of 2.5 nm each. All the emission spectra were scanned at a rate of 10 nm/min and averaged over 3 scans. The final spectrum was smoothened using adjacent-averaging available in the OriginPro Version 8.0 software. For recording ANS fluorescence intensity, the parameters were λ_{ex} = 350 nm, λ_{em} = 475 nm, excitation band pass = 2.5 nm, and emission band pass = 3 nm. Several data points at a given condition were collected to get an estimate of the standard deviation associated with the measurement. For recording Nile Red fluorescence spectra, the parameters were λ_{ex} = 560 nm, λ_{em} (scan range) = 570−690 nm, excitation band pass = 4 nm, and emission band pass = 4 nm. The graphs were plotted using commercially available OriginPro Version 8.0 software.

2.5. Circular Dichroism (CD) Spectroscopy. The CD spectra of the protein samples were recorded on a Chirascan CD spectrometer (Applied Photophysics) at ∼24 °C. Typically, for far-UV CD experiments, the protein stock solution (1 mM in pH 7, 5 mM phosphate buffer) was diluted 400-fold to a final protein concentration of 2.5 μM in the respective pH buffer, which was taken in a quartz cuvette of 2 mm path length, and the secondary structural changes were recorded in the range of 190−260 nm. The scan rate was 0.1 nm/s, and the final spectrum was averaged over 5 scans. For near-UV CD experiments, the final protein concentration was 40 μM in the respective pH buffer taken in a quartz cuvette of 10 mm path length, and the tertiary structural changes were recorded in the range of 250−350 nm. All the CD spectra were buffer subtracted using Pro-Data software provided with the Chirascan CD spectrometer. For thermal unfolding experiments using a CD spectrometer, the CD spectra of ovalbumin conformers equilibrated at different pH were collected as a function of temperature using the same parameters as discussed above. The temperature of the protein sample was varied from 25 to 90 °C using a Peltier temperature controller (Temperature Control TC125, Quantum Northwest) with a 5 min equilibration time at each temperature. All the CD spectra were plotted using the commercially available OriginPro Version 8 software and wherever required fitted using nonlinear least-square curve fitting. The goodness of the fit was determined by the adjusted R^2 value (which was typically in the range of 0.97−0.99) and the respective residual plots. To estimate the secondary structural content (percentage analysis) of different conformers of ovalbumin, the CDNN[15] program (CD spectra deconvolution software) provided with the Chirascan CD spectrometer was used.

2.6. Time-Resolved Fluorescence Measurements. Time-resolved fluorescence decay measurements of the samples were made using a picosecond laser coupled to a time-correlated single-photon-counting (TCSPC) setup. A mode-locked frequency-doubled Nd:YAG laser (Spectra Physics, U.S.) of 1 ps pulse width was used to pump a dye (Rhodamine 6G) laser, and the generated dye laser pulses were frequency doubled using a KDP crystal.[16] The samples were excited at 295 nm (for Trp) and 307 nm (for ANS). The instrument response function (IRF) was collected using a dilute colloidal suspension of dried nondairy whitener. The width of the IRF was ∼40 ps. The fluorescence emission was collected using a microchannel plate photomultiplier (Model 2809u; Hamamatsu Corp.). An emission monochromator was fixed at 350 nm with a band pass of 10 nm (for Trp) and 475 nm (for ANS). A long-pass filter (345 nm for Trp and 400 nm for ANS) was placed just after the sample to block any scattering from the sample. For anisotropy decay measurements, the emission data were collected at 0° and 90° with respect to the excitation polarization, and the anisotropy decays were analyzed by globally fitting $I_{||}(t)$ and $I_{\perp}(t)$ as follows:

$$I_{||}(t) = I(t)[1 + 2r(t)]/3 \quad (2)$$

$$I_{\perp}(t) = I(t)[1 - r(t)]/3 \quad (3)$$

$I_{\perp}(t)$ was always corrected with the G-factor. $I(t)$ is the fluorescence intensity collected at magic angle (54.7°) at time t. For lifetimes, the traces of $I(t)$ vs t were deconvoluted with respect to IRF and were analyzed by sum of exponentials using nonlinear least-square method. The anisotropy decays were analyzed using biexponential decay model describing fast and slow rotational correlation times as follows

$$r(t) = r_0[\beta_{fast} \exp(-t/\phi_{fast}) + \beta_{slow} \exp(-t/\phi_{slow})] \quad (4)$$

where r_0 is intrinsic fluorescence anisotropy, ϕ_{fast} and ϕ_{slow} are fast and slow rotational correlation times, and β_{fast} and β_{slow} are amplitudes associated with fast and slow rotational time.

The global (slow) rotational correlation time (ϕ_{slow}) is related to viscosity (η) and molecular volume (V) by the Stokes−Einstein relationship as follows

$$\phi_{slow} = \eta V/kT \quad (5)$$

$$V = \frac{4}{3}\pi R_h^3 \quad (6)$$

where R_h is the hydrodynamic radius of the molecule.

2.7. Stopped-Flow Fluorescence Experiments. The kinetics of molten-globule formation from ovalbumin at pH 2 was monitored by the change in total fluorescence intensity of tryptophan and ANS as a result of pH jump from native state (pH 7, 5 mM phosphate buffer) to the molten-globule-like state (pH 2, 50 mM KCl−HCl buffer) with a spectrometer (Chirascan, Applied Photophysics) fitted to a stopped-flow apparatus (SF.3, Applied Photophysics) equipped with a high-gain visible photomultiplier tube. Appropriate long-pass filters were used to block the scattered excitation light and allow the emission light to pass through. The protein solution under native condition (pH 7) and the required low-pH buffer (pH 2) containing ANS were rapidly mixed in 1:2.5 ratio, and the kinetics of conformational transition was monitored using a cuvette of 2 mm path length at room temperature. For monitoring tryptophan/ANS fluorescence, the final protein concentration was 10 μM. Tryptophan was excited at 290 nm with a band pass of 2 nm, and its total fluorescence emission was detected using a 320 nm long-pass filter. ANS was excited at 350 nm with a band pass of 2 nm, and its total fluorescence emission was detected using a 455 nm long-pass filter. The stopped-flow data were acquired for 1 s with 10 000 samples per point. Kinetic traces were collected 10 times in triplicate and averaged to get a satisfactory signal-to-noise ratio. The baseline was also collected with neutral pH (7, 50 mM) containing ANS under the same experimental conditions to determine the burst-phase amplitude. Each of the fluorescence traces was fitted to a biexponential function (fit range: 1−100 ms) using the Chirascan Pro-Data Software (Applied Photophysics), and the apparent relaxation times were estimated from the fit results. Recovered relaxation times varied from 1.3 to 2.2 ms (fast)

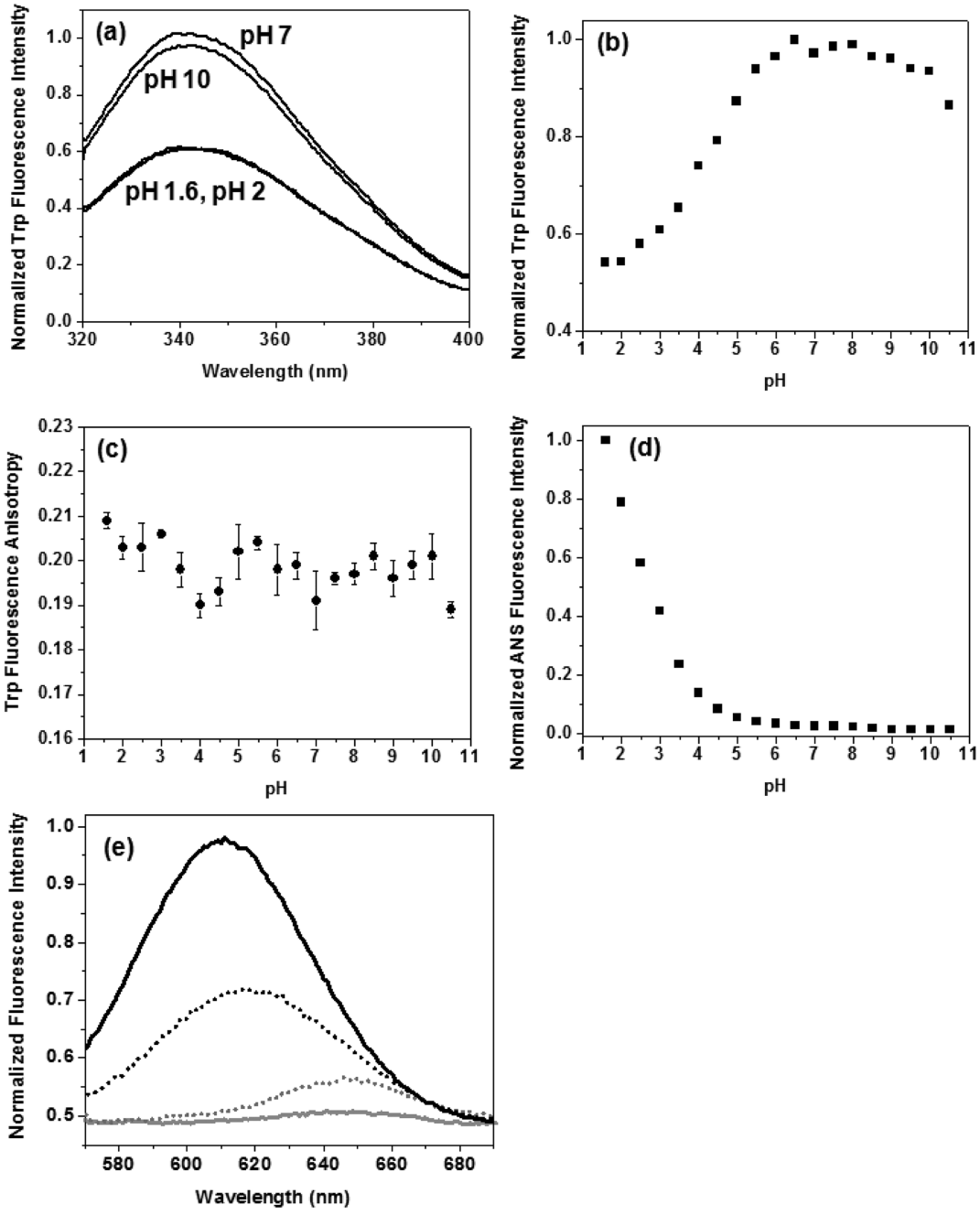

Figure 2. Variation in the (a) tryptophan fluorescence emission spectra, (b) tryptophan fluorescence intensity at 350 nm, (c) tryptophan fluorescence anisotropy, (d) ANS fluorescence intensity at 475 nm of ovalbumin conformers as a function of pH titration, and (e) Nile Red fluorescence spectra in buffers (pH 7, gray dotted line; pH 2, gray solid line) and in the presence of ovalbumin at pH 7 (black dotted line) and at pH 2 (black solid line).

and 37 to 48 ms (slow). The goodness of the fit was determined by the residual plots, and the errors associated with the relaxation times were also calculated.

3. RESULTS AND DISCUSSION

The conformational alterations in ovalbumin as a consequence of pH titration were characterized using steady-state fluorescence and CD spectroscopy. To investigate the changes in conformation and size of ovalbumin as a function of pH, the fluorescence properties of intrinsic tryptophans and extrinsic ANS (noncovalently bound to protein) were measured. Since both the fluorophores are environment-sensitive, any conformational alteration in the protein due to a change in the solution pH can be monitored by a change in the fluorescence intensity, and a shift in the emission spectrum is conveniently observed depending upon the location of the probe in either polar or nonpolar environment. Additionally, fluorescence anisotropy measurements provide information about the mobility of the fluorophore on the protein matrix and the overall size of the biomolecules.[17] To ensure that under different pH conditions ovalbumin does not form aggregates, the change in tryptophan fluorescence anisotropy was measured in a concentration-dependent manner (2−200 μM) under both native and acidic conditions. It was

dx.doi.org/10.1021/jp208416d |J. Phys. Chem. B 2012, 116, 520–531

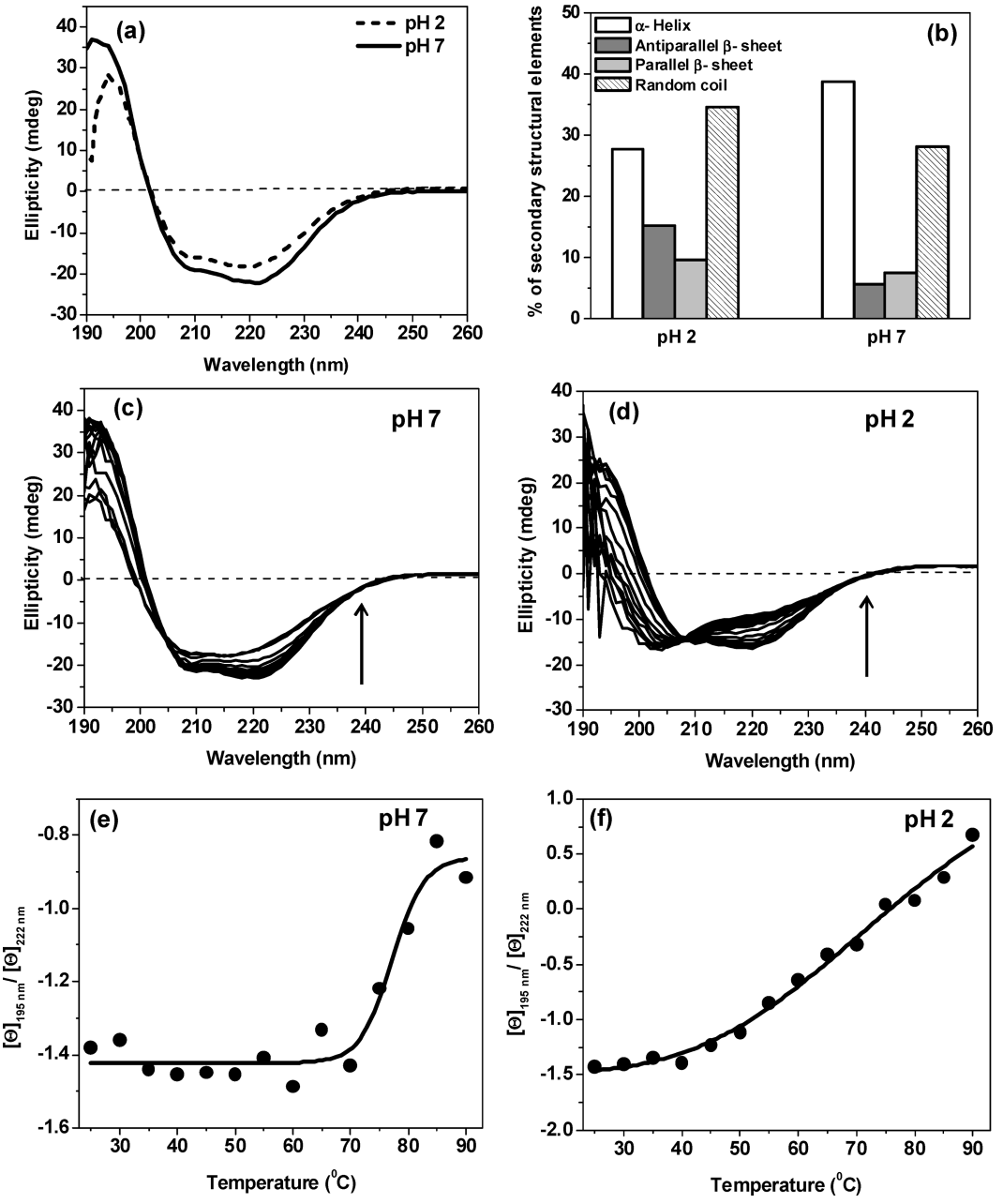

Figure 3. (a) Far-UV CD spectra of ovalbumin in the native (solid line) and molten-globule (short-dashed line) forms of ovalbumin at 25 °C. All the spectra were collected after respective baseline correction and buffer subtraction. (b) Histogram representing the percentage composition (obtained by CDNN analysis) of different secondary structural elements present in both native (pH 7) and molten-globule-like state (pH 2) of ovalbumin. (c, d) Thermal unfolding of ovalbumin (from 25 to 90 °C; indicated by an upward arrow) of native (pH 7) and partially expanded (pH 2) states. (e, f) Plots of ratiometric ellipticities (filled circle) at 195 nm (random-coil) vs 222 nm (α-helix) of ovalbumin at (e) pH 7 and (f) pH 2 as a function of temperature. The black line in both the plots represents the fit obtained using sigmoidal function available in the Origin software.

observed that the tryptophan anisotropy remains constant in a concentration range of 2−50 μM at both low and neutral pH. Hence, all the fluorescence measurements were carried out at a protein concentration of 10 μM where ovalbumin remains predominantly monomeric (see Experimental Methods). Moreover, in order to monitor the changes in secondary structural elements of ovalbumin as a function of both pH and temperature, far-UV CD spectra were collected and the percentage compositions of the secondary structural elements were also determined (see Experimental Methods).

3.1. Steady-State Fluorescence Studies as a Function of pH: Conformational Transition. At pH 7, the tryptophans of the native ovalbumin exhibited a maximum fluorescence emission at ~345 nm. As the pH was lowered, a progressive decrease in the tryptophan fluorescence intensity was observed (Figure 2a) while the emission maximum remained unchanged. This could be ascribed to the loss in tertiary structure that probably results in a partial unfolding leading to tryptophan fluorescence quenching by water molecules. Changing the pH toward the alkalinity resulted in a very slight decrease in the tryptophan intensity

dx.doi.org/10.1021/jp208416d |J. Phys. Chem. B 2012, 116, 520–531

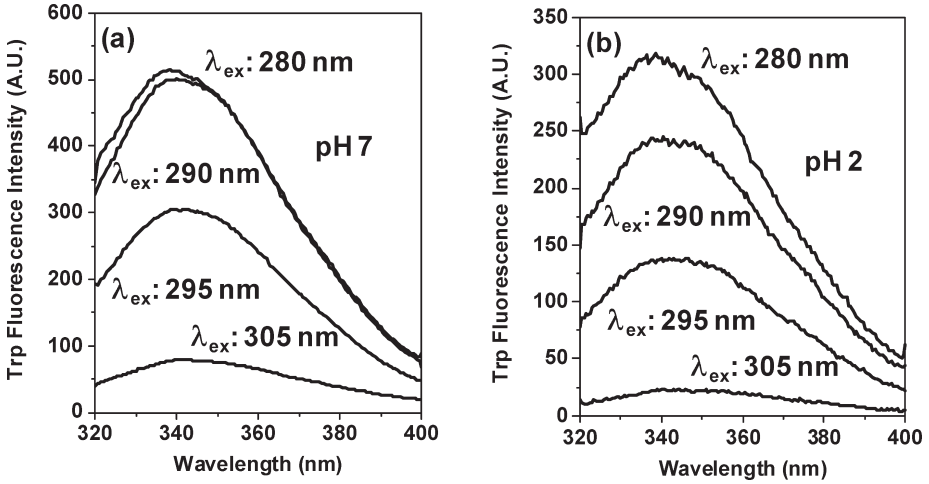

Figure 4. Red-edge excitation shift (REES) of intrinsic tryptophans (without intensity-normalized at respective emission maximum) observed in (a) native (at pH 7) and (b) molten-globule-form (at pH 2) of ovalbumin as a function of excitation wavelengths, viz., 280, 290, 295, and 305 nm. As the excitation wavelength is shifted toward the red edge of tryptophan absorption band, a moderate red shift in the tryptophan emission is also observed. Each spectrum is an average of three scans, and the individual final spectrum was smoothed using adjacent-averaging available in the Origin software.

(Figure 2a) compared to that observed at neutral pH with no apparent shift in the emission maximum. Therefore, according to the tryptophan intensity pattern at 350 nm as a function of pH (Figure 2b), the ovalbumin conformers could be possibly classified into two major conformational states, namely, an acid-induced partially unfolded form and a predominantly native, compact form thus portraying an apparent two-state transition. Additionally, the steady-state fluorescence anisotropy of the tryptophan residues was measured during the pH titration experiments (Figure 2c). The tryptophan fluorescence anisotropy measured (0.21 ± 0.002) in the acidic pH regime was slightly higher than that observed in the neutral and alkaline pH (0.19 ± 0.005) indicating a conformational expansion in the low-pH molten-globule form. The change in the anisotropy of ovalbumin was much smaller compared to that of serum albumin upon conversion into a low-pH molten-globule-like form.[18] Taken together, both the fluorescence intensity and anisotropy data indicate that ovalbumin forms a partially unfolded conformer at low pH. We would like to point out that steady-state anisotropy often does not provide unambiguous assignments of local flexibility and size since local and global dynamics are averaged out. In order to distinguish size changes from local flexibility change, we have carried out picosecond time-resolved fluorescence anisotropy measurements (see later in section 3.4).

Since molten-globule states are associated with exposed hydrophobic patches and the low pH-form of ovalbumin has been shown to bind to ANS,[12] we carried out ANS-binding studies of ovalbumin as a function of pH. ANS is weakly fluorescent in aqueous environment but fluoresces strongly (with a concurrent blue shift in its emission maximum from ~510 to ~475 nm) when bound to hydrophobic pockets.[19] It was observed that ANS fluorescence intensity at 475 nm decreased progressively as the pH of the medium was increased from acidic to neutral and further to basic (Figure 2d). Therefore, ANS-binding experiments indicated the transition from native to molten-globule form of ovalbumin at low pH. Since ovalbumin is positively charged at pH 2 and can interact with the negatively charged ANS, we have also studied binding experiments with a neutral dye, namely, Nile Red, that has been previously used to detect molten-globule states of other proteins.[20−22] Nile Red fluorescence demonstrated significant increase in fluorescence intensity with a concomitant blue shift to ~610 nm compared to that of the native protein (Figure 2e). All of the above experiments indicated the presence of hydrophobic pockets in the acid-induced conformational state of ovalbumin.

3.2. CD Spectroscopy: Changes in the Secondary and Tertiary Structures. It was inferred from tryptophan, ANS, and Nile Red fluorescence intensity pattern that ovalbumin forms a partially unfolded molten-globule conformer at low pH. Following these observations, we performed far-UV CD experiments to further investigate and analyze the secondary structural content of ovalbumin at both low and neutral pH. It has been earlier demonstrated that ovalbumin forms a molten-globule-like state at acidic pH and largely retains its secondary structure.[11,12] As expected, a moderate reduction in the helicity was observed at pH 2 compared to the native form of ovalbumin at pH 7 (Figure 3a). Comparison of the near-UV CD spectra of the pH-induced conformational isomers corroborated the same trend; rather at pH 2, a significant loss in tertiary structure was observed as reported earlier.[12] Analysis of the secondary structural content of the native and molten-globule-like conformers yielded the percentage composition of the individual secondary structural elements (Figure 3b). A considerable increase in both β-sheet and random-coil structures at the expense of the α-helices in the molten-globule form is observed compared to that in the native form. Next, we embarked upon investigating the thermal unfolding behavior of both native and molten-globule states. As the temperature was increased, a progressive dissolution of the secondary structural elements was observed for both native and molten-globule like states (Figures 3c, d). At pH 7, a sharp change in the secondary structure was observed at ~75 °C indicating a cooperative transition, whereas at pH 2, more gradual structural loss was observed (Figure 3e, f; also see Figures S1 and S2). This observation again corroborates the fact that at pH 2 ovalbumin forms partially unfolded molten-globule-like states with a reduction in the secondary and tertiary structures that may account for its more gradual structural loss upon thermal unfolding. Such weakly cooperative unfolding transitions have

dx.doi.org/10.1021/jp208416d | J. Phys. Chem. B 2012, 116, 520–531

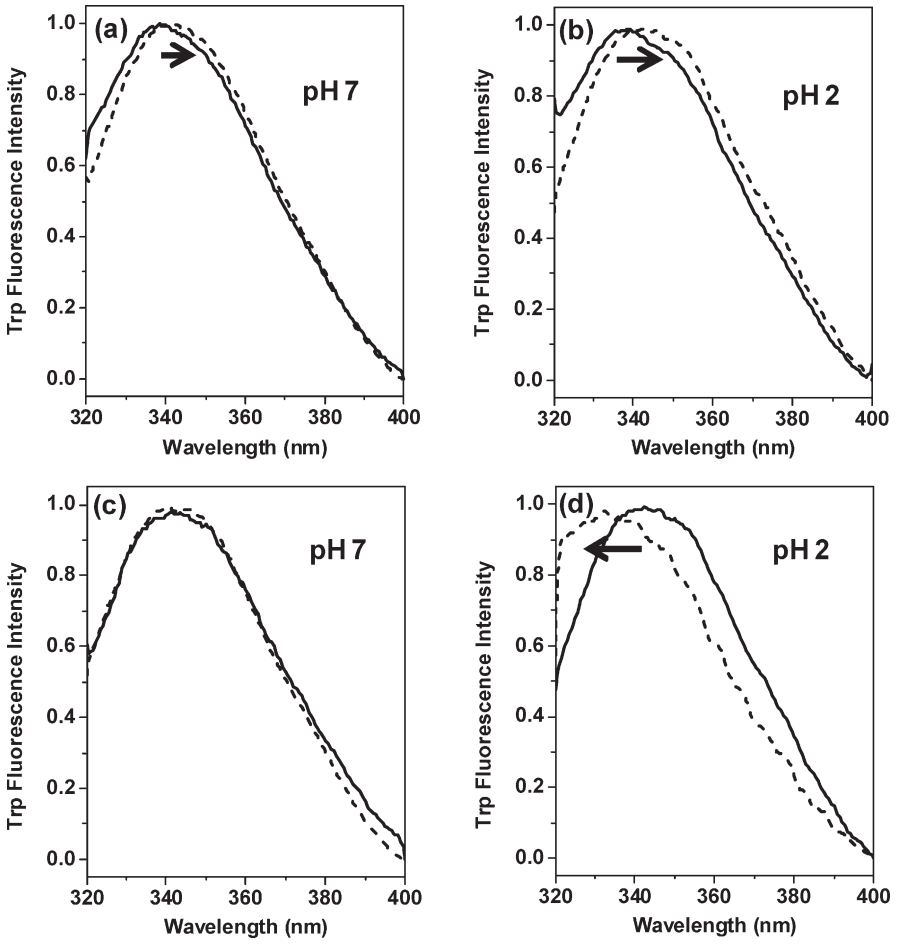

Figure 5. Fluorescence emission spectra of intrinsic tryptophans of both native (pH 7) and molten-globule (pH 2) states of ovalbumin in the absence and presence of a quencher. (a, b) REES in the absence of a quencher as a function of excitation wavelength; the solid line and the short-dashed line are the tryptophan emission spectra at λ_{ex} = 280 and 295 nm, respectively. (c, d) Tryptophan emission spectra of ovalbumin at pH 7 and pH 2 as a function of quencher (KI) concentration (varied from 0 to 500 mM) at a constant excitation wavelength of 295 nm. Two representative spectra are shown here at KI concentration of 0 mM (solid line) and 300 mM (short-dashed line). In all cases, each spectrum is an average of three scans and the individual final spectrum was intensity-normalized at its maximum for better visualization and smoothed using the adjacent-averaging algorithm available in the Origin software.

been earlier observed for a number of small proteins that demonstrate downhill protein folding.[23−26]

3.3. Red-Edge Excitation Shift (REES): Microenvironment and Dipolar Relaxation around Intrinsic Tryptophan Residues. After characterization of the molten-globule-like state of ovalbumin at pH 2 using CD, tryptophan, and ANS fluorescence, we further extended our studies to investigate the dielectric relaxation of the hydration shell surrounding the intrinsic tryptophans using red-edge excitation shift (REES) for both expanded and native conformers. Generally, REES is observed when the fluorophore is placed in a viscous or moderately viscous medium.[27−29] Due to the solvent viscosity, the motion of the solvent molecules around the excited fluorophore is restrained which slows down the rate of solvent relaxation and is generally comparable or longer than the fluorescence lifetime. Therefore, when the excitation wavelength is gradually shifted toward the red edge of the fluorophore absorption, a progressive red shift in the fluorophore emission maximum as a function of the shift in the excitation wavelength is observed which is denoted as REES. It has been demonstrated that REES offers direct information about the dynamics of the solvent shell around a polar fluorophore and has been successfully utilized in probing the organization and dynamics of membrane proteins.[28,29] In our study, we observed a moderate shift in the intrinsic tryptophan maximum as a function of change in the excitation wavelength toward the red edge under different pH conditions (Figure 4). When the excitation wavelength was changed from 280 to 305 nm, the tryptophan emission maximum shifted from 338 to 345 nm (7 nm shift). Interestingly, the extent of REES in tryptophan emission remained unchanged under all pH conditions from pH 1.6 to 10 (Figures 4 and S3). Figures 5a and b show normalized tryptophan fluorescence spectra at two different excitation wavelengths (280 and 295 nm) which allow better visual comparison of REES. Such moderate shifts in tryptophan emission maximum in both molten-globule and native state have been reported recently for soluble proteins[30,31] indicating that the motion of the solvent molecules around the excited tryptophans are restricted and the extent of shift was found to vary in different conformations as expected. However, in our case, the degree of shift in tryptophan emission was observed to be similar and independent of the ovalbumin conformational state (native and molten-globule). Interpretation of REES for multi-tryptophan proteins has always been complicated due to possible differences in the

Table 1. Typical Parameters Associated with Time-Resolved Fluorescence Intensity and Anisotropy Decays of Tryptophan and ANS in Native and Molten-Globule Forms of Ovalbumin

	fluorescence lifetime in ns (amplitude)			mean lifetime in ns		rotational correlation times in ns [a] (amplitude)				
conditions (fluorophore)	τ_1 (α_1)	τ_2 (α_2)	τ_3 (α_3)	τ_m	χ^2	ϕ_{fast} (β_{fast})	ϕ_{slow} (β_{slow})	r_0	r_{ss}	χ^2
native (tryptophan)	0.54 (0.38)	2.28 (0.29)	6.54 (0.33)	3.04	1.02	0.29 (0.22)	14.86 (0.78)	0.191	0.119	1.88
molten-globule (tryptophan)	0.51 (0.38)	2.29 (0.38)	4.99 (0.24)	2.27	1.02	0.24 (0.25)	21.41 (0.76)	0.214	0.144	1.33
molten-globule (ANS)	1.1 (0.14)	6.47 (0.38)	15.8 (0.48)	10.2	0.99	0.11 (0.59)	23.7 (0.41)	0.160	0.043	1.16

[a] The errors associated with the rotational correlation times and their amplitudes: (a) For native (tryptophan): $\phi_{fast} = 0.24 \pm 0.05$ ns, $\beta_{fast} = 0.24 \pm 0.03$; $\phi_{slow} = 14.1 \pm 1.2$ ns, $\beta_{slow} = 0.76 \pm 0.03$. (b) For molten-globule (tryptophan): $\phi_{fast} = 0.22 \pm 0.02$ ns, $\beta_{fast} = 0.26 \pm 0.03$; $\phi_{slow} = 21.6 \pm 0.7$ ns, $\beta_{slow} = 0.74 \pm 0.03$. (c) For molten-globule (ANS): $\phi_{fast} = 0.11 \pm 0.04$ ns, $\beta_{fast} = 0.60 \pm 0.03$; $\phi_{slow} = 24.1 \pm 0.8$ ns, $\beta_{slow} = 0.40 \pm 0.03$. Estimated hydrodynamic volumes are as follows: 69.1 ± 5.5 nm^3 (native); 96.7 ± 3.2 nm^3 (molten-globule using tryptophan); 110.5 ± 3.7 nm^3 (molten-globule using ANS).

microenvironment of tryptophan residues.[31] In other words, different exposure levels of tryptophan residues in a multitryptophan protein could lead to the REES effect without slow dipolar relaxation. Therefore, in order to distinguish between multiple environments and slow dipolar relaxation around tryptophan at both low and neutral pH, we carried out fluorescence quenching experiments. We hypothesized that if the tryptophans are distributed in two distinct environments (buried and exposed) as a consequence of pH-induced conformational transitions, addition of a quencher such as KI to the protein solution would quench the fluorescence emanating from the more exposed tryptophan(s) whereas the fluorescence from the more buried tryptophans will remain unchanged. As a result, the contribution of the buried tryptophan to the observed fluorescence intensity will become prominent with an increase in quencher concentration, and a blue shift in the tryptophan emission will be observed at a constant excitation wavelength. However, if there is no observed spectral shift as the quencher is added, then the observed REES under identical solution condition is indeed due to dipolar relaxation around the tryptophan residues.

To test our hypothesis, we carried out quenching experiments where KI was used as the quencher and its concentration was varied from 0 to 500 mM. At a constant excitation wavelength of 295 nm and at pH 7, the tryptophans of the native protein did not show any shift in the emission maximum (Figure 5c) even at the highest KI concentration of 500 mM. In contrast, at the same excitation wavelength and at pH 2 (where ovalbumin exists as a molten-globule), the tryptophan emission maximum showed a progressive blue shift of ~11 nm (from ~344 to ~333 nm), and a rapid decrease in tryptophan intensity at 350 nm was observed with an increase in KI concentration (Figure 5d). Therefore, from the quenching experiments, it was inferred that the REES observed in the native protein is likely due to slow dipolar relaxation around the tryptophans which are present in a viscous microenvironment. Our inference is further supported by the crystallographic data on ovalbumin[9] wherein a large number of hydrogen-bonded water molecules in the immediate vicinity of an α-helix (harboring W148) and a few β-strands (of the central β-sheet containing W184) were observed (Figure 1c). Extensive hydrogen-bonding network between the water molecules, described as "the greatest density of ordered water",[9] is present in the aforementioned region that explains the viscous surroundings around the tryptophans and the REES observed at neutral pH. However, at pH 2, the formation of molten-globule-like state may result in partial unfolding due to which the tryptophan residues might be distributed in different environments. Therefore, at low pH, the observed 7 nm shift may be due to environmental heterogeneity of the tryptophan residues rather than the slow dipolar relaxation. However, we do not entirely rule out the possibility of slow dipolar relaxation in the molten-globule form at pH 2.

3.4. Time-Resolved Fluorescence Measurements: Insights into the Structure and Dynamics. In order to gain more dynamical insights into the nature of the native as well as the low-pH molten-globule state of ovalbumin, we have carried out picosecond time-resolved fluorescence measurements. Tryptophan showed three fluorescence lifetime components both in native and in low-pH state. The longest lifetime component and the associated amplitude in the native form (~6.5 ns, 33%) decreased considerably in the low-pH form (~5 ns, 24%) whereas the other two shorter lifetime components (~2.3 and ~0.5 ns) remained largely unchanged (Table 1; Figures 6a, b). The mean fluorescence lifetime of tryptophan decreased from ~3 ns (native) to ~2.3 ns (molten-globule). This is expected since the partially expanded, molten-globule form allows water molecules to permeate the protein which results in the decrease in the tryptophan fluorescence lifetime.[32] Next, we performed tryptophan fluorescence anisotropy decay measurements to investigate the dynamics and dimension of different forms of ovalbumin. The time-resolved fluorescence anisotropy decay measurements allow one to separate the local and global dynamics of a fluorophore attached to a biomolecule which is clearly reflected in different rotational correlation times (ϕ_{fast} and ϕ_{slow}).[17,33] Global dynamics is represented by the slow rotational correlation time (ϕ_{slow}) that is generally related to the size (hydrodynamic volume) of the protein (eqs 5, 6 in Experimental Methods). In our experiments, the fast and slow rotational correlation times of ovalbumin in the native state were found to be ~0.2 and ~14 ns, respectively (Table 1; Figure 6c). Subsequently, the mean hydrodynamic radius was determined to be ~2.6 nm which shows a good agreement with the R_h value (2.67 nm) calculated using an empirical relationship.[34] For the molten-globule form, the fast and slow rotational correlation times were recovered to be ~0.2 and ~21 ns, respectively (Table 1; Figure 6d). The slow rotational correlation time (representing the global dynamics of the protein) of the molten-globule state is longer than that of the native form indicating an expansion in the former that results in a slower tumbling motion of the protein and, hence, slower fluorescence depolarization. Since tryptophan fluorescence lifetime (2.3 ns) is considerably shorter than the long rotational correlation time in the low-pH form, the precision in the estimation of the long rotational correlation time is likely to be poor. Therefore, we have also used ANS that is known to have much longer fluorescence lifetime (>10 ns) when bound to hydrophobic pockets.[17]

dx.doi.org/10.1021/jp208416d | J. Phys. Chem. B 2012, 116, 520–531

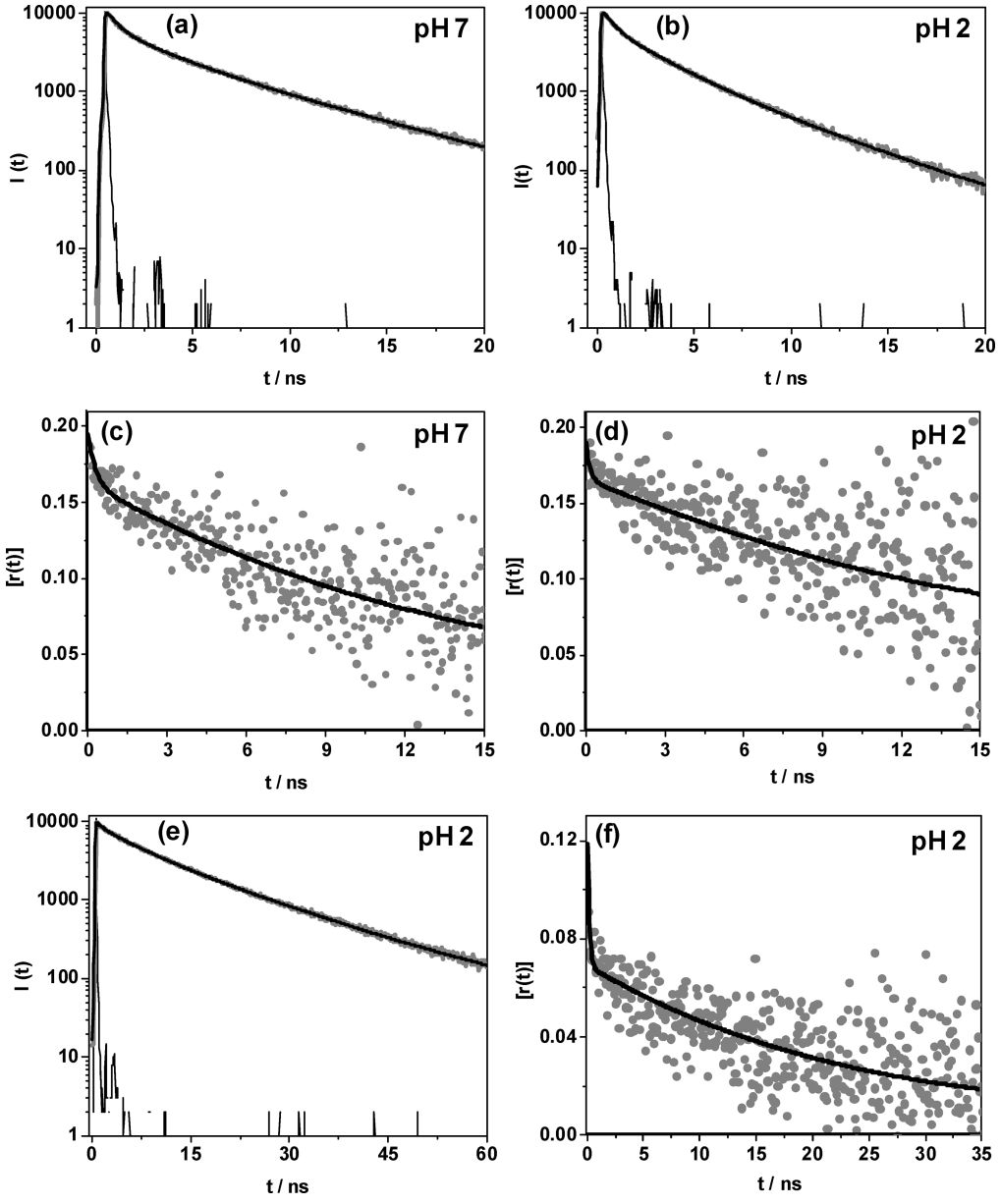

Figure 6. Time-resolved fluorescence decay profiles of ovalbumin in the native (pH 7) and molten-globule (pH 2) forms. (a, b) Tryptophan fluorescence intensity decay plots of native and molten-globule states of ovalbumin, respectively, at room temperature. (c, d) Tryptophan fluorescence anisotropy decays of ovalbumin in the native and molten-globule conformations, respectively. (e) Time-resolved fluorescence intensity decay and (f) time-resolved fluorescence anisotropy decay of ANS bound to the molten-globule state of ovalbumin at pH 2. In all the fluorescence intensity decay plots, the sharp, thin black lines represent the instrument response function, the gray lines represent the observed intensity decay, and black lines correspond to the fits obtained using a triexponential function. In all the fluorescence anisotropy decay plots, the gray filled circles represent the observed anisotropy decays, and the black lines represent the fits obtained using a biexponential function.

In the low-pH molten-globule state of ovalbumin, ANS showed much longer mean lifetime of ~10 ns (Table 1; Figure 6e). Fluorescence anisotropy decay measurements on ANS bound to molten-globule state of ovalbumin demonstrated a long rotational correlation time of ~24 ns that further supports our observation of conformational expansion in the molten-globule state of the protein (Table 1; Figure 6f). In summary, our time-resolved fluorescence anisotropy results indicated that the hydrodynamic volume increased ~40% (from ~70 nm^3 for native to ~100 nm^3 for molten-globule) which is in accordance with the size expansion of 35−60% in archetypal molten-globules.[1,35]

3.5. Stopped-Flow Kinetics of ANS Fluorescence: Formation of Molten-Globule from the Native Form. After establishing that ovalbumin forms conformationally expanded molten-globule-like state at pH 2 with enhanced hydrophobicity and ANS binding ability, we next investigated the kinetics of conformational transition upon pH jump from the native state (pH 7) to the molten-globule state (pH 2) using stopped-flow fluorescence technique. The time-dependent increase in total ANS fluorescence intensity was used as a read-out to monitor the kinetics of molten-globule formation.[36−38] Upon rapidly jumping the pH from 7 to 2, the total ANS fluorescence intensity

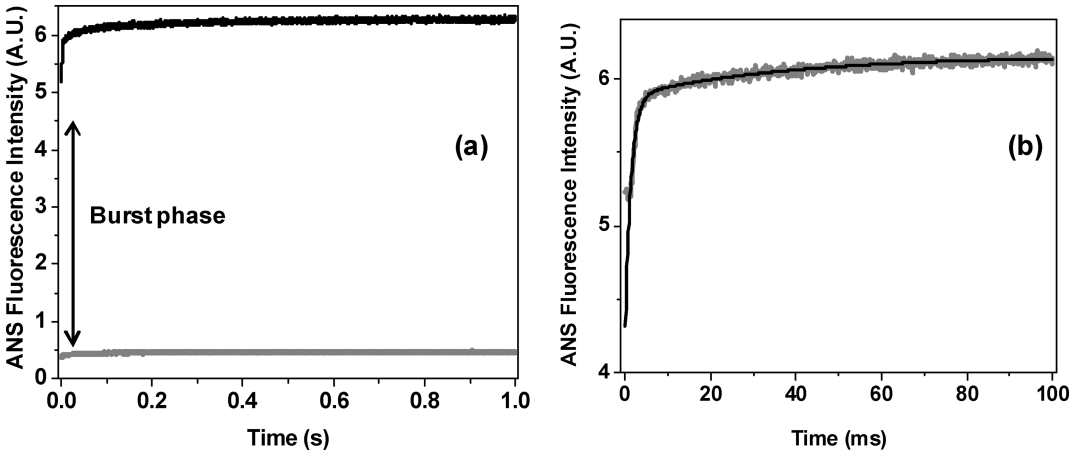

Figure 7. Stopped-flow fluorescence kinetics. (a) Time-dependent change in the total ANS fluorescence intensity observed upon pH jump from native state (pH 7) to the molten-globule-like state (pH 2) of ovalbumin at room temperature using stopped-flow fluorescence technique. The native baseline is shown in gray. (b) The rise in ANS fluorescence (gray line) could be satisfactorily fitted (black line) to a double-exponential function. Two apparent relaxation times were recovered from the fit (1.3 ± 0.1 and 37.7 ± 5.9 ms).

Scheme 1. Mechanism of Formation of Low pH Molten-Globule State from Native Ovalbumin

$$N \xrightarrow{< 1\ ms} [I_1] \xrightarrow{\sim 2\ ms} [I_2] \xrightarrow{\sim 40\ ms} MG$$

showed a fast increase within the dead time of mixing with a burst-phase of over 70% (Figure 7a). The amplitude of burst-phase was similar for stopped-flow kinetics of intrinsic tryptophan fluorescence (Figure S4). A large amplitude of burst-phase indicates that the major phase in the molten-globule formation involves (fast) submillisecond conformational change that is the key characteristic of downhill folders.[39,40] The analysis of ANS fluorescence kinetic traces revealed that the conformational change from the native to the molten-globule-like state is a biphasic process consisting of a fast phase followed by a slow phase (Figure 7b). The time constant of the fast phase is ∼2 ms, whereas the slow phase of conformational reorganization occurs with a relaxation time of ∼40 ms. Our kinetic results are consistent with a mechanistic outline that is presented in Scheme 1 that describes a stepwise formation of the molten-globule (MG) state of ovalbumin involving a burst-phase with a submillisecond conformational change followed by slower biphasic conformational reorganizations on the millisecond time scale leading to the final molten-globule state.

4. CONCLUSIONS

In summary, the present work describes a systematic and detailed characterization of the molten-globule-like state of ovalbumin formed at low pH using steady-state and time-resolved fluorescence spectroscopy. Also, we observed REES of ∼7 nm for tryptophan in the native ovalbumin which implies that the rate of reorientation of the hydration shell around the excited tryptophans is slow, thus indicative of a "motionally restricted" microviscous environment around the tryptophans due to the presence of highly ordered water molecules in the vicinity of the tryptophans. In the molten-globule form, REES could arise due to microenvironmental heterogeneity. The analysis of time-resolved tryptophan fluorescence anisotropy decays further supported the conformational expansion of ∼40% upon molten-globule formation at pH 2. Additionally, upon pH jump from 7 to 2, stopped-flow ANS fluorescence kinetics revealed that the formation of molten-globule state is a multistep process which, indeed, involves a rapid submillisecond conformational change followed by a biphasic slower reorganization that occurs on the milliseconds time scale leading to the formation of the final molten-globule form. It is interesting to note the weakly cooperative thermal unfolding behavior coupled with the fast submillisecond formation, and the acid-induced molten-globule state of ovalbumin might share some features of downhill folding proteins. Since the molten-globule formation and fast-folding are likely to be governed by similar physical principles, it would be interesting and worthwhile to establish a connection between these two distinct folding regimes. Very recently, the connection between downhill folding and molten-globule formation has been addressed using atomistic and coarse-grained simulations.[41] Understanding the key structural and dynamical features of molten-globule state of proteins will be of significant interest in the current context of protein misfolding and aggregation. We believe that the low-pH, partially expanded, molten-globule conformer comprising exposed hydrophobic regions of ovalbumin might serve as a precursor to amyloid aggregates that might have important implications in the study of serpin polymerization related to serpinopathies.

■ ASSOCIATED CONTENT

Supporting Information. Thermal unfolding using CD, REES at different pH, and stopped-flow tryptophan fluorescence kinetics of ovalbumin (Figures S1−S4). This material is available free of charge via the Internet at http://pubs.acs.org.

■ AUTHOR INFORMATION

Corresponding Author

*E-mail mily@iisermohali.ac.in (M.B.), mukhopadhyay@iisermohali.ac.in (S.M.); tel. +91-172-224-0209; fax +91-172-224-0266.

■ ACKNOWLEDGMENT

We thank the members of the Mukhopadhyay lab for critically reading the manuscript. M.B. thanks the Department of Science and Technology (DST), New Delhi for the Women Scientists' grant. S.M. thanks the Council of Scientific and Industrial Research (CSIR), New Delhi for a research grant. We thank Prof. G. Krishnamoorthy and Ms. M. Kombrabail (TIFR Mumbai) for helping us with the time-resolved fluorescence measurements and Prof. N. Periasamy (TIFR Mumbai) for providing us with the time-resolved fluorescence data analysis software.

■ REFERENCES

(1) Ptitsyn, O. B. Molten globule and protein folding. *Adv. Protein Chem.* **1995**, *47*, 83–229.

(2) Jahn, T. R.; Radford, S. E. Folding vs aggregation: Polypeptide conformations on competing pathways. *Arch. Biochem. Biophys.* **2008**, *469*, 100–117.

(3) Luheshi, L. M.; Crowther, D. C.; Dobson, C. M. Protein misfolding and disease: From the test tube to the organism. *Curr. Opin. Chem. Biol.* **2008**, *12*, 25–31.

(4) Gooptu, B.; Lomas, D. A. Conformational pathology of the serpins: Themes, variations and therapeutic strategies. *Annu. Rev. Biochem.* **2009**, *78*, 147–176.

(5) Kaiserman, D.; Whisstock, J. C.; Bird, P. I. Mechanisms of serpin dysfunction in disease. *Expert Rev. Mol. Med.* **2006**, *8*, 1–19.

(6) Stein, P.; Chothia, C. Serpin tertiary structure transformation. *J. Mol. Biol.* **1991**, *221*, 615–621.

(7) Mine, Y. Recent advances in the understanding of egg white protein functionality. *Trends Food Sci. Technol.* **1995**, *6*, 225–232.

(8) Broersen, K.; Teeffelen, A. M. M. V.; Vries, A.; Voragen, A. G. J.; Hamer, R. J.; Jongh, H. H. J. D. Do sulfhydryl groups affect aggregation and gelation properties of ovalbumin? *J. Agric. Food Chem.* **2006**, *54*, 5166–5174.

(9) Stein, P. E.; Leslie, A. G. W.; Finch, J. T.; Carrell, R. W. Crystal structure of uncleaved ovalbumin at l.95 Å resolution. *J. Mol. Biol.* **1991**, *221*, 941–959.

(10) Donnell, E. R.-O. The ovalbumin family of serpin proteins. *FEBS Lett.* **1993**, *315*, 105–108.

(11) Koseki, T.; Kitabatake, N.; Doi, E. Conformational changes in ovalbumin at acid pH. *J. Biochem.* **1988**, *103*, 425–430.

(12) Tatsumi, E.; Hirose, M. Highly ordered molten globule-like state of ovalbumin at acidic pH: Native-like fragmentation by protease and selective modification of Cys367 with dithiopyridine. *J. Biochem.* **1997**, *122*, 300–308.

(13) Tatsumi, E.; Yoshimatsu, D.; Hirose, M. Conformational state of ovalbumin at acidic pH as evaluated by a novel approach utilizing intrachain sulfhydryl-mixed disulfide exchange reactions. *Biochemistry* **1998**, *37*, 12351–12359.

(14) Naeem, A.; Khan, T. A.; Muzaffar, M.; Ahmad, S.; Salemuddin, M. A partially folded state of ovalbumin at low pH tends to aggregate. *Cell Biochem. Biophys.* **2011**, *59*, 29–38.

(15) Böhm. G. CDNN: CD Spectra Deconvolution, Version 2.1, 1997.

(16) Goel, T.; Mukherjee, T.; Rao, B. J.; Krishnamoorthy, G. Fluorescence dynamics of double and single stranded DNA bound to histone and micellar surfaces. *J. Phys. Chem. B* **2010**, *114*, 8986–8993.

(17) Lakowicz, J. R. *Principles of fluorescence spectroscopy*, 3rd ed.; Springer: New York, 2006.

(18) Bhattacharya, M.; Jain, N.; Bhasne, K.; Kumari, V.; Mukhopadhyay, S. pH-Induced conformational isomerization of bovine serum albumin studied by extrinsic and intrinsic protein fluorescence. *J. Fluoresc.* **2011**, *21*, 1083–1090.

(19) Daniel, E.; Weber, G. Cooperative effects in binding by bovine serum albumin I: The binding of 1-anilino-8-naphthalenesulfonate fluorimetric titrations. *Biochemistry* **1966**, *5*, 1893–1900.

(20) Polverini, E.; Cugini, G.; Annoni, F.; Abbruzzetti, S.; Viappiani, C.; Gensch, T. Molten globule formation in apomyoglobin monitored by the fluorescent probe Nile Red. *Biochemistry* **2006**, *45*, 5111–5121.

(21) Sackett, D. L.; Wolff, J. Nile red as a polarity-sensitive fluorescent probe of hydrophobic protein surfaces. *Anal. Biochem.* **1987**, *167*, 228–234.

(22) Hendriks, J.; Gensch, T.; Hviid, L.; van der Horst, M. A.; Hellingwerf, K. J.; van Thor, J. J. Transient exposure of hydrophobic surface in the photoactive yellow protein monitored with Nile red. *Biophys. J.* **2002**, *82*, 1632–1643.

(23) Garcia-Mira, M. M.; Sadqi, M.; Fischer, N.; Sanchez-Ruiz, J. M.; Muñoz, V. Experimental identification of downhill protein folding. *Science* **2002**, *298*, 2191–2195.

(24) Muñoz, V.; Sanchez-Ruiz, J. M. Exploring protein folding ensembles: A variable-barrier model for the analysis of equilibrium unfolding experiments. *Proc. Natl. Acad. Sci. U.S.A.* **2004**, *101*, 17646–17651.

(25) Oliva, F. Y.; Muñoz, V. A simple thermodynamic test to discriminate between two-state and downhill folding. *J. Am. Chem. Soc.* **2004**, *126*, 8596–8597.

(26) Sanchez-Ruiz, J. M. Probing free-energy surfaces with differential scanning calorimetry. *Annu. Rev. Phys. Chem.* **2011**, *62*, 231–255.

(27) Demchenko, A. P. The red-edge effects: 30 years of exploration. *Luminescence* **2002**, *17*, 19–42.

(28) Raghuraman, H.; Kelkar, D. A.; Chattopadhyay, A. Novel insights into protein structure and dynamics utilizing the red edge excitation shift approach. In *Reviews in Fluorescence*; Geddes, C. D., Lakowicz, J. R., Eds.; Springer, New York, 2005; pp 199—222.

(29) Haldar, S.; Chaudhuri, A.; Chattopadhyay, A. Organization and dynamics of membrane probes and proteins utilizing the red edge excitation shift. *J. Phys. Chem. B* **2011**, *115*, 5693–5706.

(30) Chattopadhyay, A.; Rawat, S. S.; Kelkar, D. A.; Ray, S.; Chakrabarti, A. Organization and dynamics of tryptophan residues in erythroid spectrin: Novel structural features of denatured spectrin revealed by the wavelength-selective fluorescence approach. *Protein Sci.* **2003**, *12*, 2389–2403.

(31) Kelkar, D. A.; Chaudhuri, A.; Haldar, S.; Chattopadhyay, A. Exploring tryptophan dynamics in acid-induced molten-globule state of bovine α-lactalbumin: A wavelength-selective fluorescence approach. *Eur. Biophys. J.* **2010**, *39*, 1453–1463.

(32) De Lauder, W. B.; Wahl, P. H. Effect of solvent upon the fluorescence decay of indole. *Biochim. Biophys. Acta* **1971**, *243*, 153–163.

(33) Saxena, A.; Udgaonkar, J. B.; Krishnamoorthy, G. In *Applications of Fluorescence Spectroscopy*; Hof, M., Hutterer, R., Fidler, V., Eds.; Springer-Verlag: New York, 2005.

(34) Wilkins, D. K.; Grimshaw, S. B.; Receveur, V.; Dobson, C. M.; Jones, J. A.; Smith, L. J. Hydrodynamic radii of native and denatured proteins measured by pulse field gradient NMR techniques. *Biochemistry* **1999**, *38*, 16424–16431.

(35) Kharakoz, D. P.; Bychkova, V. E. Molten globule of human a-lactalbumin: hydration, density and compressibility of the interior. *Biochemistry* **1997**, *36*, 1882–1890.

(36) Hawe, A.; Sutter, M.; Jiskoot, W. Extrinsic fluorescent dyes as tools for protein characterization. *Pharm. Res.* **2008**, *25*, 1487–1499.

(37) Semisotnov, G. V.; Rodionova, N. A.; Razgulyaev, O. I.; Uversky, V. N.; Gripas, A. F.; Gilmanshin, R. I. Study of the "molten globule" intermediate state in protein folding by a hydrophobic fluorescent probe. *Biopolymers* **1991**, *31*, 119–128.

(38) Paolo, A. D.; Balbeur, D.; Pauw, E. D.; Redfield, C.; Matagne, A. Rapid collapse into a molten globule is followed by simple two-state kinetics in the folding of lysozyme from bacteriophage λ. *Biochemistry* **2010**, *49*, 8646–8657.

(39) Li, P.; Oliva, F. Y.; Naganathan, A. N.; Muñoz, V. Dynamics of one-state downhill protein folding. *Proc. Natl. Acad. Sci. U.S.A.* **2009**, *106*, 103–108.

(40) Naganathan, A. N.; Li, P.; Perez-Jimenez, R.; Sanchez-Ruiz, J. M.; Muñoz, V. Navigating the downhill protein folding regime via structural homologues. *J. Am. Chem. Soc.* **2010**, *132*, 11183–11190.

(41) Naganathan, A. N.; Orozco, M. The native ensemble and folding of a protein molten-globule: Functional consequence of downhill folding. *J. Am. Chem. Soc.* **2011**, *133*, 12154–12161.